JACS
JOURNAL OF THE AMERICAN CHEMICAL SOCIETY
pubs.acs.org/JACS
Article

Copper-Catalyzed Transfer Hydrodeuteration of Aryl Alkenes with Quantitative Isotopomer Purity Analysis by Molecular Rotational Resonance Spectroscopy

Zoua Pa Vang,[‖] Albert Reyes,[‖] Reilly E. Sonstrom, Martin S. Holdren, Samantha E. Sloane, Isabella Y. Alansari, Justin L. Neill, Brooks H. Pate, and Joseph R. Clark*

Cite This: *J. Am. Chem. Soc.* 2021, 143, 7707−7718

Read Online

ACCESS | Metrics & More | Article Recommendations | Supporting Information

ABSTRACT: A copper-catalyzed alkene transfer hydrodeuteration reaction that selectively incorporates one hydrogen and one deuterium atom across an aryl alkene is described. The transfer hydrodeuteration protocol is selective across a variety of internal and terminal alkenes and is also demonstrated on an alkene-containing complex natural product analog. Beyond using ^{1}H, ^{2}H, and ^{13}C NMR analysis to measure reaction selectivity, six transfer hydrodeuteration products were analyzed by molecular rotational resonance (MRR) spectroscopy. The application of MRR spectroscopy to the analysis of isotopic impurities in deuteration chemistry is further explored through a measurement methodology that is compatible with high-throughput sample analysis. In the first step, the MRR spectroscopy signatures of all isotopic variants accessible in the reaction chemistry are analyzed using a broadband chirped-pulse Fourier transform microwave spectrometer. With the signatures in hand, measurement scripts are created to quantitatively analyze the sample composition using a commercial cavity enhanced MRR spectrometer. The sample consumption is below 10 mg with analysis times on the order of 10 min using this instrument—both representing order-of-magnitude reduction compared to broadband MRR spectroscopy. To date, these measurements represent the most precise spectroscopic determination of selectivity in a transfer hydrodeuteration reaction and confirm that product regioselectivity ratios of >140:1 are achievable under this mild protocol.

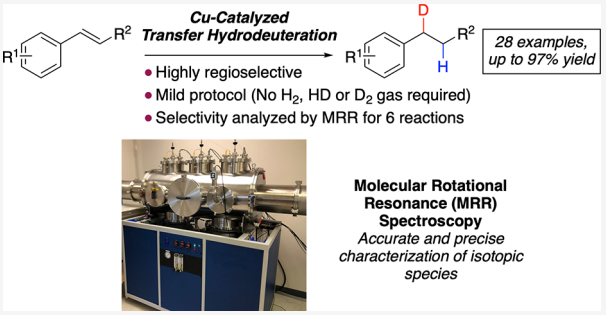

1. INTRODUCTION

Reactions that incorporate deuterium into molecular scaffolds are of topical relevance to scientists across several disciplines. Among many applications, deuterated small molecules are used as standards for high-resolution mass spectrometry[1−3] and can serve as probes to study reaction mechanisms,[4,5] perform kinetic isotope effect experiments,[6,7] determine the stereochemical course of microbiological or enzymatic reactions, and elucidate biosynthetic pathways.[8−17] Importantly, deuterated small molecules are also deployed to alter absorption, distribution, metabolism, and excretion (ADME) properties of drug molecules.[18,19] Consequently, designing deuterated bioisosteres to modify the metabolic "soft spots" of small molecule drugs holds much potential for the development of safer therapeutics.[20−24]

Transition metal catalyzed reactions are commonly used to selectively install oxygen, nitrogen, or carbon functionality into small molecules.[25,26] Mild protocols and modular catalytic frameworks are often exploited in these reactions to optimize both reactivity and selectivity. However, highly selective transition metal catalyzed methods for deuterium incorporation remain underdeveloped. For example, transition metal catalyzed hydrogen isotope exchange (HIE) reactions efficiently incorporate deuterium into small molecules, but significant challenges exist to control the quantity and precise placement of deuterium in a given molecule.[27,28] Specific to making small molecules with one deuterium atom installed at a benzylic carbon, a general technique to access small molecules with a benzylic $C(sp^2)$−D bond was recently reported.[29] However, to make a small molecule with exactly one benzylic $C(sp^3)$−D bond, chemists typically use reactions involving stoichiometric organometallic intermediates.[30]

The similar physical properties of deuterium relative to hydrogen further complicate unselective deuteration reactions. Isotopic mixtures are not only inseparable using common purification techniques, but common spectroscopic techniques used to characterize organic compounds are insufficient at measuring the precise location and quantity of deuterium in

Received: January 23, 2021
Published: May 17, 2021

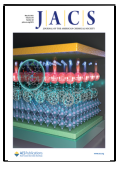

https://doi.org/10.1021/jacs.1c00884
J. Am. Chem. Soc. 2021, 143, 7707−7718

isotopic product mixtures. This can have major implications in drug discovery, and guidance to address deuterated active pharmaceutical ingredients (APIs) is being developed for these spectroscopic and synthetic challenges.[31] Ultimately, synthetic access to deuterated compounds free of isotopic impurities and analytical methods to identify all isotopic species in a product mixture will be crucial for developing novel deuterated APIs.

Catalytic transfer hydrogenations represent powerful and mild methods for the reduction of alkene functionality.[32−35] We believe that mechanistically similar catalytic transfer hydrodeuteration reactions hold much promise for making selectively deuterated small molecules. Until recently, selective catalytic hydrodeuteration reactions were rare and usually employed as mechanistic probes for alkyne semireductions.[36−38] A major challenge in catalytic transfer hydrodeuteration is discriminating between hydrogen (H) and deuterium (D) for selective incorporation into alkene functionality.[39,40] Catalytic alkene transfer hydrodeuteration reactions are now possible on a variety of alkenes.[41−45] Transition metal catalyzed transfer hydrodeuteration typically occurs in a regioselective manner for unactivated terminal alkenes, but selectivity is generally lower for terminal aryl alkene substrates (Scheme 1a).[41−43] Alternatively, using a boron catalyst, highly selective installation of deuterium into activated 1,1-diarylalkenes is possible, but with a limited alkene scope (Scheme 1b).[44,45]

Scheme 1. Transfer Hydrodeuteration of Alkenes

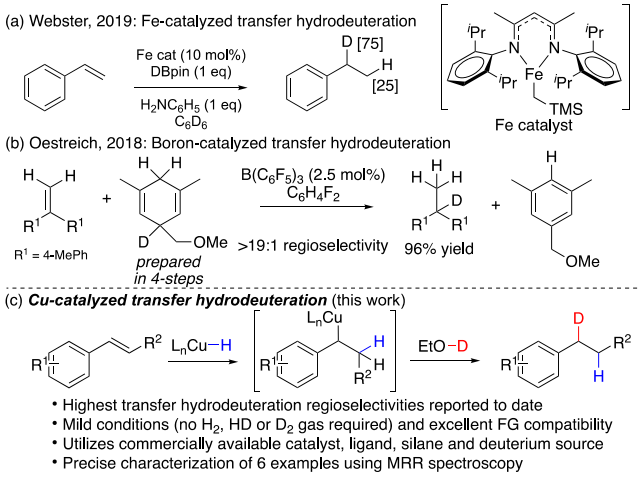

2. REACTION OPTIMIZATION AND SCOPE

Based on insight gleaned from our recently published Cu-catalyzed regioselective aryl alkyne transfer hydrodeuteration studies, we hypothesized that a highly regioselective aryl alkene transfer hydrodeuteration may be possible (Scheme 1c).[46] Cu-catalyzed aryl alkene hydroamination reactions are also regioselective, and we envisioned the transfer hydrodeuteration occurring with excellent regioselectivity because of the thermodynamic favorability of the benzylic copper intermediate depicted in Scheme 1c.[47−51] Under transfer hydrodeuteration conditions, we reasoned that the H-donor and D-donor would operate at distinct points during the reaction and therefore allow for precise insertion of each atom at the desired location within the aryl alkene.

Accordingly, *tert*-butyldimethylsilyl-protected (TBS) cinnamyl alcohol *trans*-**1** was chosen as the aryl alkene for reaction optimization. In the presence of catalytic $Cu(OAc)_2$, dimethoxymethylsilane (DMMS was chosen for the optimization studies because it can be easily removed under vacuum during product purification), and EtOD, we found that bidentate bisphosphine ligands such as DPPE, DPPF, *rac*-BINAP, and DPPBz were not efficient at supporting the desired transformation (Table 1, entries 1−4). Switching to

Table 1. Reaction Optimization[a]

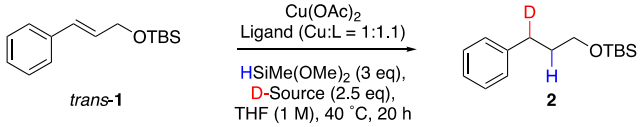

entry	$Cu(OAc)_2$	ligand	D-source	**1** (%)	**2**(%)
1	2 mol %	**L1**	EtOD	69[b]	–
2	2 mol %	**L2**	EtOD	70[b]	–
3	2 mol %	**L3**	EtOD	89[b]	–
4	2 mol %	**L4**	EtOD	47[b]	–
5	2 mol %	**L5**	EtOD	–	85[c]
6	2 mol %	**L5**	MeOD	8[c]	69[c]
7	2 mol %	**L5**	D_2O	59[c]	21[c]
8	1 mol %	**L5**	IPA-d_8	–	85[c]
9	1 mol %	**L5**	EtOD	–	90[c]

[a]Reactions conducted using 0.2 mmol of substrate. $Cu(OAc)_2$ was used as a 0.2 M solution in THF. [b]Yield was determined by ^1H NMR analysis of the crude reaction mixture, using mesitylene as an internal standard. [c]Denotes isolated product yield.

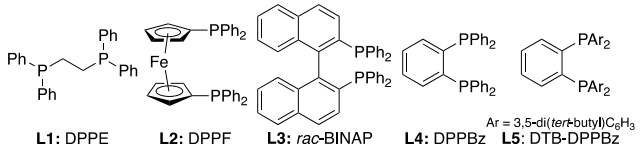

the more sterically crowded DTB-DPPBz ligand dramatically affected reactivity, and deuterated aryl alkane **2** was isolated in 85% yield (entry 5). Importantly, evaluation of the product by ^1H, ^2H, and ^{13}C NMR revealed that one deuterium atom was incorporated exclusively at the benzylic position (>20:1 regioselective ratio). Varying the deuterium source revealed that using CH_3OD led to a slight decrease in yield (entry 6), while D_2O only led to partial conversion to product **2** (entry 7). Employing 2-propanol-d_8 permitted the catalyst loading to be lowered and was similarly efficient as EtOD (entry 8). Ultimately, returning to the reaction conditions from entry 5 and decreasing the catalyst loading to 1 mol % was found to be optimal (entry 9).

With the optimal reaction conditions in hand, we evaluated the substrate scope of the reaction (Scheme 2). Electron-rich monosubstituted alkenyl arenes containing oxygen functionality performed well in the reaction, and excellent yields of the desired deuterated products were obtained (Scheme 2a, **4a**−**4d**, 73−97% yield). Alternatively, an alkenyl arene substituted with an electron-withdrawing nitro group also underwent transfer hydrodeuteration to provide the deuterated aryl alkane, albeit in moderate yield (**4e**, 47% yield). Nitrogen substitution is permitted on the alkenyl arene substrate (**4f**−**4g**, 57−97% yield). Importantly, we demonstrated that polymethylhydrosiloxane could be used instead of DMMS in the synthesis of **4g**. We also found that (4-vinylphenyl)boronic acid pinacol ester can undergo Cu-catalyzed transfer hydrodeuteration (**4h**, 67% yield).

https://doi.org/10.1021/jacs.1c00884
J. Am. Chem. Soc. 2021, 143, 7707−7718

Scheme 2. Aryl Alkene Transfer Hydrodeuteration Substrate Scope

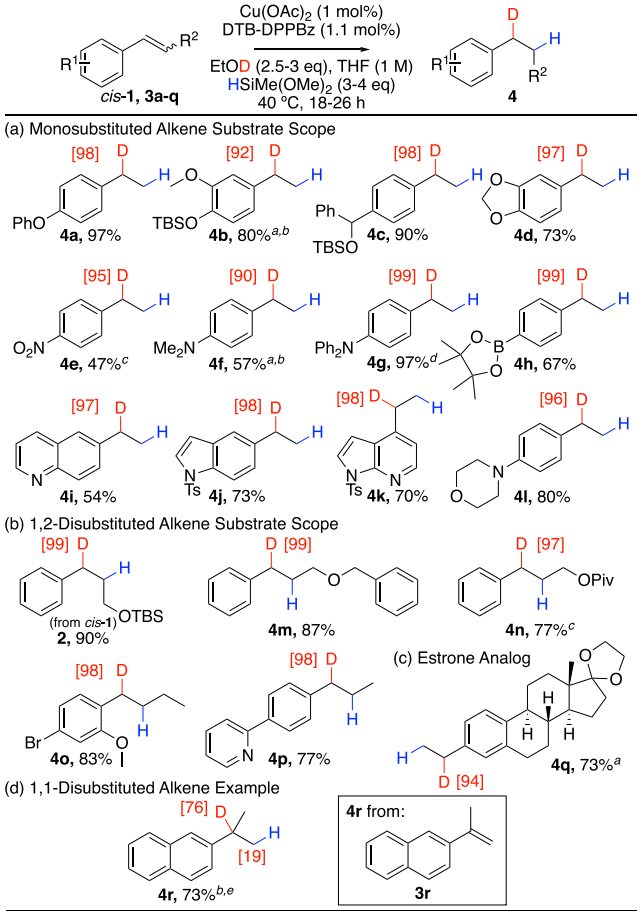

[a]2 mol % $Cu(OAc)_2$ and 2.2 mol % DTB-DPPBz used. [b]IPA-d_8 (3 equiv) used instead of EtOD. [c]Reaction conducted at 5 °C. [d]Polymethylhydrosiloxane (3 equiv) used instead of $HSiMe(OMe)_2$. [e]3 mol % $Cu(OAc)_2$, 3.3 mol % DTB-DPPBz, and $HSiMe(OMe)_2$ (4 equiv) used at 60 °C.

Due to their prevalence in bioactive molecules, nitrogen- and oxygen-containing heterocycles were examined under the transfer hydrodeuteration protocol.[52,53] We found that quinoline, indole, and azaindole substituted alkenes perform well in the transfer hydrodeuteration reaction (**4i**−**4k**, 54−73% yield). Alternatively, an alkenyl arene substituted with a morpholine ring is efficiently converted to the deuterated aryl alkane product (**4l**, 80% yield). Internal alkene substrates are also viable candidates for transfer hydrodeuteration. Cinnamyl alcohol derivatives were evaluated when the alcohol was protected with a TBS, benzyl (Bn), or pivaloyl (Piv) group (Scheme 2b). All three derivatives were deuterated in high yield (**2**, **4m**−**4n**, 77−90% yield). Notably, product **2** was synthesized from the *cis*-alkene starting material, whereas in Table 1 it was synthesized from the *trans*-alkene starting material. Substitution on the arene is also possible for internal alkene substrates. A bromine substituted alkenyl arene and pyridine substituted alkenyl arene underwent transfer hydrodeuteration in high yield (**4o**−**4p**, 77−83% yield). Notably, no dehalogenation product was observed in the synthesis of **4o**. We also explored the capacity for the Cu-catalyzed transfer hydrodeuteration to proceed in a complex small molecule setting (Scheme 2c). Accordingly, a vinyl substituted estrone analog was deuterated in good yield (**4q**, 73% yield). Lastly, we evaluated the transfer hydrodeuteration reaction selectivity for a 1,1-disubstituted aryl alkene (Scheme 2d). The reaction of **3r** was only moderately selective with deuterium incorporation favoring the benzylic position (4:1 benzylic:methyl selectivity). We attribute the moderate selectivity to the demanding steric environment of this 1,1-disubstituted alkene inhibiting the Cu-catalyst from approaching the benzylic site.

The alkenyl arene transfer hydrodeuteration scope was extended, and the resulting isotopic products were analyzed using molecular rotational resonance (MRR) spectroscopy (Scheme 3; see below for analysis details). In addition to a vinyl biphenyl substrate, polyaromatic compounds such as 2-vinylnaphthalene and 2-methoxy-6-vinylnaphthalene were readily converted to their corresponding deuterated products (**6a**−**c**, 83−91% yield). Heterocycle-containing aryl alkenes and an internal alkene were also evaluated under the transfer hydrodeuteration protocol (**6d**−**6f**, 76−86% yield). In all six examples, the major products (**6a**−**f**) were formed in high yield in a highly regioselective manner. In addition to providing higher sensitivity measurements for isotopic product analysis, using MRR to analyze the reaction products depicted in Scheme 3 further validates our claims that this reaction is highly regioselective. It removes any ambiguity when analyzing isotopic product mixtures consisting of isotopologues and isotopomers that share deuterium substitution at the same atom, such that several isotopic species contribute to the same $^1H/^2H$ resonance in an NMR spectrum. It also precisely quantifies each regioisomer, even when the d_0-species is present in the product mixture.

To demonstrate the versatility of the reaction, we hypothesized that flipping the regioselectivity of the reaction would be possible by simply replacing the Si−H and EtOD with Si−D and EtOH. This was examined with vinyl biphenyl substrate **5a** (Scheme 4a) and resulted in an 80% yield of desired product **7a**. An increase of the "underdeuterated" transfer hydrogenation side product **8a** was observed in this

Scheme 3. Substrate Scope Analyzed by Molecular Rotational Resonance

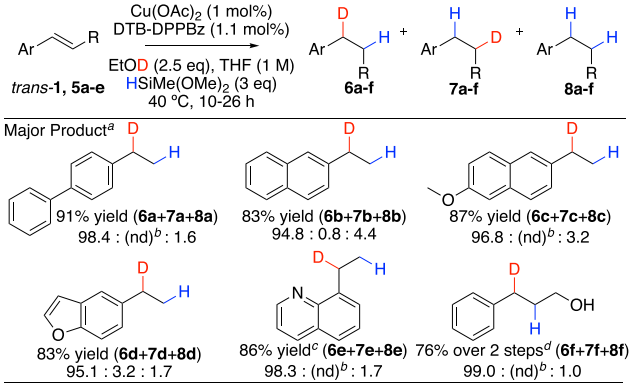

[a]The major products were **6a**−**f**, the product distribution was determined by MRR, and the ratio represents the ratio of all products in the product mixture (**6a**−**f**:**7a**−**f**:**8a**−**f**) after purification. [b]Compound not detected (nd) by ^2H NMR or MRR. See Supporting Information (SI) for detection limits. [c]2 mol % $Cu(OAc)_2$ and 2.2 mol % DTB-DPPBz were used. [d]Transfer hydrodeuteration product was purified then subjected to TBS deprotection.

https://doi.org/10.1021/jacs.1c00884
J. Am. Chem. Soc. 2021, 143, 7707−7718

Scheme 4. Reaction Studies

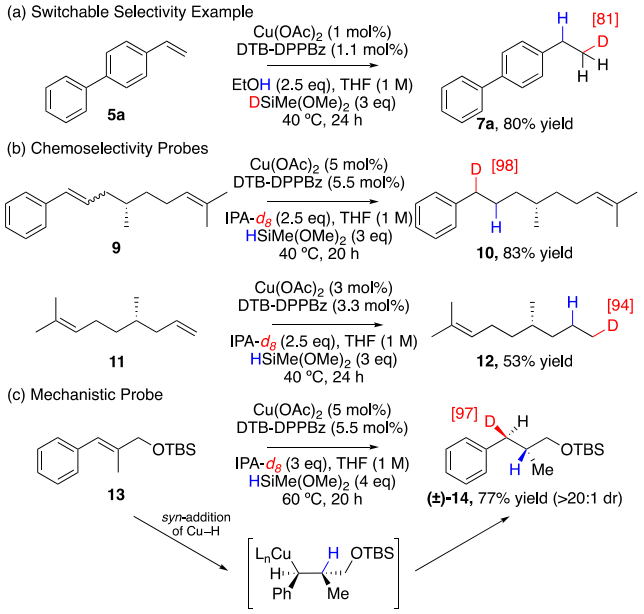

reaction likely because of the reduced deuterium content in the Si–D reagent.

To probe the chemoselectivity of the reaction, we performed the transfer hydrodeuteration on a substrate containing both a 1,2-disubstituted styrenyl alkene and 1,1,2-trisubstituted alkene (Scheme 4b, substrate **9**). We were pleased to find the reaction was not only highly selective for incorporation of deuterium at the benzylic site of **10** but also chemoselective, as no reduction of the 1,1,2-trisubstituted alkene was observed. Another chemoselectivity probe was carried out using substrate **11**. In this case, the chemoselective reaction of an unactivated terminal alkene was evaluated in the presence of a more sterically hindered internal alkene. Furthermore, substrate **11** evaluated the potential for an unactivated alkene to undergo regioselective Cu-catalyzed transfer hydrodeuteration using the DTB-DPPBz ligand. Isolation of deuterated product **12** revealed that the reaction was highly selective for copper inserting into the less sterically hindered terminal position of the terminal alkene, as no reduction of the trisubstituted alkene was observed. Ongoing studies in our research group are underway to explore the scope of the Cu-catalyzed alkene transfer hydrodeuteration for unactivated alkenes. Lastly, we probed whether the selectivity of the Cu–H insertion into the alkene occurred with *syn*- or *anti*-addition using 1,2,2-trisubstituted alkene **13**. We isolated product **(±)-14** in 77% yield (>20:1 dr) which suggests that *syn*-addition of the Cu–H across the alkene is operative (Scheme 4c). Furthermore, this example also indicates that trisubstituted alkenes are viable substrates for regioselective transfer hydrodeuteration.

3. SPECTROSCOPIC ANALYSIS OF PRODUCTS

Quantitative Sample Analysis by Molecular Rotational Resonance Spectroscopy – A New Tool for Deuteration Chemistry. The isotopic composition of the reaction products depicted in Scheme 3 was analyzed by molecular rotational resonance (MRR) spectroscopy. The measurements provide high resolution and specificity for the analysis of isotopic species and represent the first quantitative assessment of the MRR spectroscopy technique for deuterated impurity analysis. In MRR spectroscopy, the rotational spectrum arises through electric-dipole transitions between the quantized rotational kinetic energy levels of the molecule.[54] In the rigid rotor approximation, the energy levels can be calculated from the three rotational constants (A, B, C) derived from the moments-of-inertia for rotation about the three principal rotational axes (I_A, I_B, I_C)

$$A = (\hbar^2/2)I_A^{-1} \tag{1}$$

where the moment-of-inertia is calculated from the nuclear masses and the shortest distance of each nucleus to the rotation axis.

$$I_A = \sum_i m_i r_{A_i}^2 \tag{2}$$

The intensities for the rotational transitions are governed by the electric dipole moment, and the molecule must be polar to have a rotational spectrum.

MRR spectroscopy provides measurement solutions for several of the challenges that have been highlighted for the analysis of deuterated molecules.[31] The important feature of rotational spectroscopy in this application is that each isotopic variant has its own unique spectral signature. In particular, isotopomers have distinct MRR spectra and can be separately analyzed within a complex mixture.[55] By comparison, mass spectrometry can only analyze the isotopologue composition. NMR spectroscopy also has limitations and cannot perform the composition analysis when isoptologues and isotopomers in the mixture share deuterium substitution at the same atom such that several isotopic species contribute to the same $^1H/^2H$ resonance. MRR spectroscopy has two additional advantages in this application. First, MRR spectroscopy has exceptionally high spectral resolution so that spectral overlap is not an issue even for complex mixtures. Second, the rotational spectrum for any isotopic variant can be predicted to high accuracy using the equilibrium geometry obtained from quantum chemistry so that high-confidence identification of isotopic species is possible without the need for reference samples.[55−57]

For the products depicted in Scheme 3, the rotational spectrum was measured using a broadband chirped-pulse Fourier transform microwave (CP-FTMW) spectrometer operating in the 2−8 GHz frequency range.[58−60] The broadband spectral coverage makes it possible to capture enough of the rotational spectrum to obtain a highly characteristic spectral pattern for each isotopic variant of the analyte present in the sample. The adiabatic expansion of a dilute mixture of the analyte in neon (0.1% mixture) into the spectrometer vacuum chamber produces a cold gas with a rotational temperature of about 1 K. The cooling of the gas increases the measurement sensitivity through reduction of the partition function. The reduced Doppler broadening of the pulsed jet expansion produces a high-resolution spectrum (line width of about 70 kHz fwhm). This feature is crucial in isotopologue/isotopomer analysis because it is not possible to separate the different species by chromatography to simplify the analysis.[61] CP-FTMW instruments have a large linear dynamic range so that quantitative analysis can be performed using the spectral transition intensities even for trace impurities.[58]

In the Cu-catalyzed transfer hydrodeuteration reaction, a possible impurity is the "misdeuterated" reaction product that

https://doi.org/10.1021/jacs.1c00884
J. Am. Chem. Soc. 2021, 143, 7707−7718

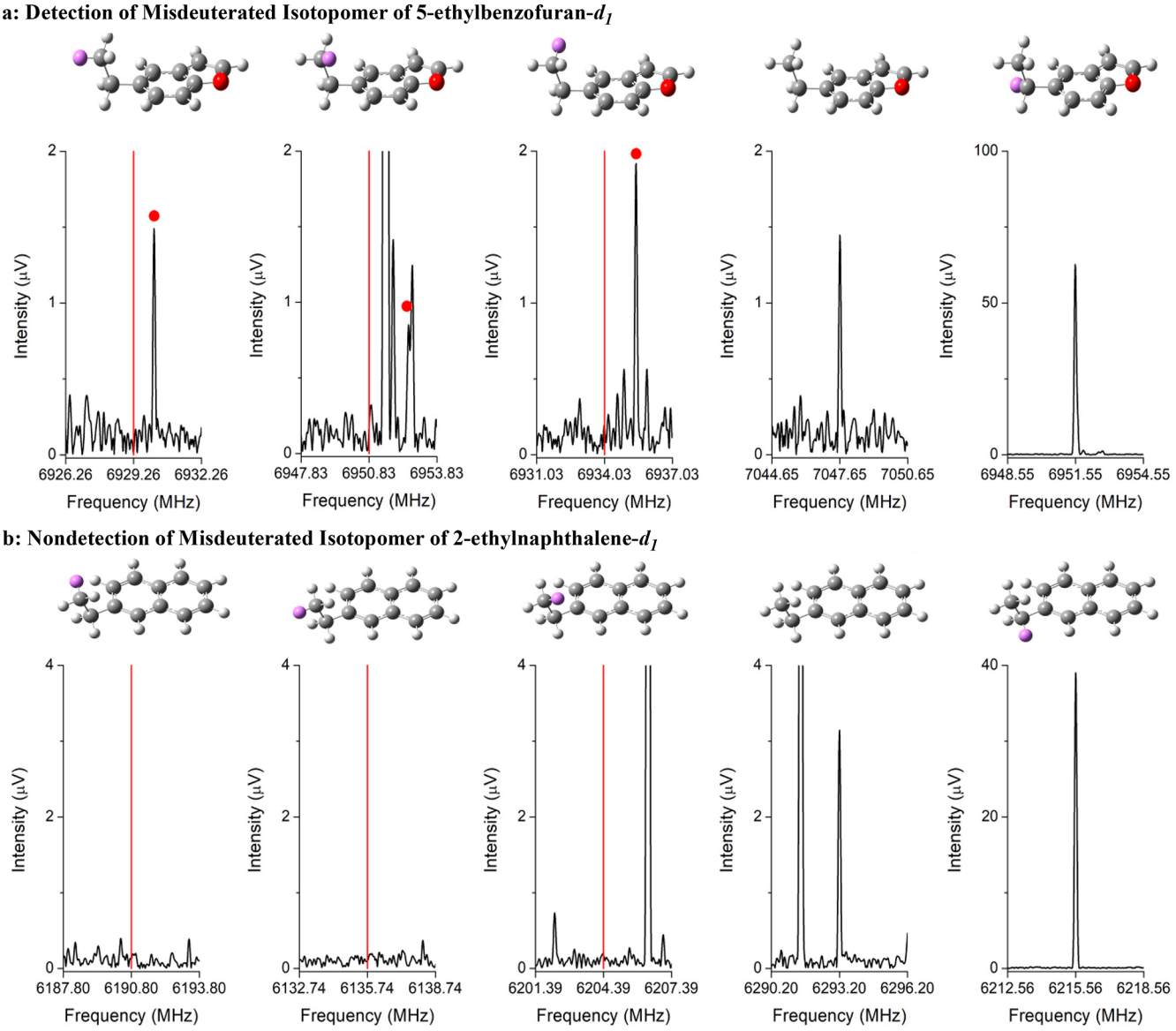

Figure 1. The isotopologue and isotopomer analysis of two of the reaction products is illustrated. Part (a) shows the analysis of the 5-ethylbenzofuran-d_1 sample (**6d**, **7d**, **8d**). The first three panels show a 6 MHz window of the rotational spectrum centered on the predicted transition frequency for the strongest transition in the spectrum (also marked by the vertical red line). The conformers of the d_1-methyl isotopomer give different spectra and the deuteration position for each transition is denoted by the purple colored atom in the structure above the spectral region. A transition assigned to each isotopomer rotational spectrum is observed and marked by the red dot. The fourth panel is centered on the observed frequency of the underdeuterated isotopologue. The fifth panel shows the rotational transition for one of the two conformers of the desired isotopomer of 5-ethylbenzofuran-d_1 (note the change in the intensity axis scale). Part (b) shows the same analysis using the strongest rotational transition of 2-ethylnaphthalene-d_1 (**7b**). In this case, no transitions in the prediction window for the misdeuterated isotopomer can be assigned to rotational spectra. The lack of detection of any rotational transitions is used to derive the upper limit to misdeuterated 2-ethylnaphthalene-d_1 reported in the SI.

results from deuterium inserting at the homobenzylic position and hydrogen at the benzylic position (minor product **7** in Scheme 3). The reaction is also expected to produce "underdeuterated" reaction product where there is no deuterium incorporation (minor product **8** in Scheme 3). This reaction product is expected from the hydrogen impurities in the alcohol-OD or trace H_2O in the alkenyl arene substrate, silane, and alcohol-OD. An overview of the MRR analysis for two of the reaction products is shown in Figure 1. The top panel of images shows narrow regions of the measured spectrum where the strongest transition in the rotational spectrum of different isotopic variants of 5-ethylbenzofuran (**6d**, **7d**, **8d**) are expected. The dominant isotopic species in the sample is the desired reaction product **6d** as indicated by the strong observed transition in the rotational spectrum assigned to this isotopomer. The attribution of the observed spectrum to the specific isotopomer is based on the agreement between experimental and theoretical rotational constants. For the transfer hydrodeuteration of 5-vinylbenzofuran, the underdeuterated impurity **8d** is also observed.

In the case of the misdeuterated reaction product **7d**, three equal intensity rotational spectra are expected from the conformational isomers of this isotopomer. The first three

https://doi.org/10.1021/jacs.1c00884
J. Am. Chem. Soc. 2021, 143, 7707−7718

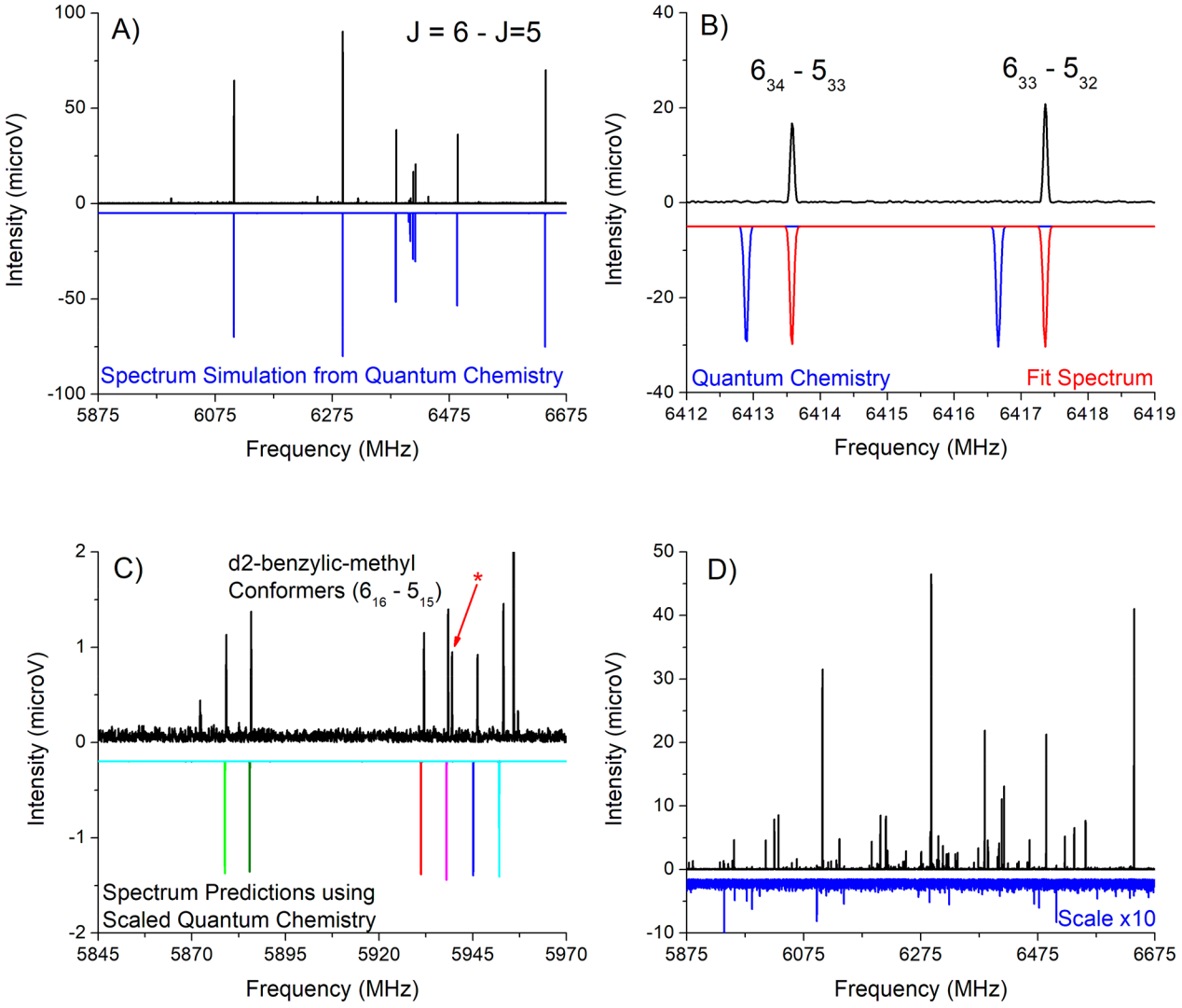

Figure 2. Portrayed above is the predicted and experimental analysis of the 2-ethylnaphthalene product mixture from the cocktail reaction and the method for analyzing the reaction product mixture when a near 1:1 mixture of H and D-reagents is used in the Cu-catalyzed transfer hydrogenation/deuteration reaction. Panels A and B show the basic MRR analysis process for a commercial sample of 2-ethylnaphthalene-d_0. The simulation of the spectrum from quantum chemistry (blue) is used to guide an experimental fit of the rotational constants (Panel B, red) of the spectrum. The results from this initial fit are used to make scaled predictions for the rotational constants for other isotopic species. The predicted transitions for the six conformers of the d_2-benzylic-methyl isotopomer are shown in Panel C. The transition marked with a red asterisk is unassigned. All strong transitions are assigned to four chemical species (d_0, d_1-benzylic, d_1-methyl, d_2-benzylic-methyl), and no further species could be identified in the residuals of the reaction product mixture spectrum shown in Panel D (blue, with the intensity multiplied by a factor of 10).

spectral regions shown in Figure 1a are 6 MHz frequency bandwidth windows centered on the predicted transition frequency obtained using the quantum chemistry equilibrium geometry calculated using the B3LYP density functional theory with Grimme's D3 dispersion correction including Becke–Johnson damping and the 6-311++G(d,p) basis set model chemistry in Gaussian16.[62] The transitions marked by the red dot are assigned to the rotational spectra of the three conformers of the d_1-methyl isotopomer. The conformational geometry associated with the spectral transition is indicated by the purple atom in the molecular structure shown above the section of the spectrum. The ^{2}H NMR spectrum of the ethylbenzofuran sample is shown in the Supporting Information (SI), and the resonance for the methyl group is barely detectable. The MRR measurement has about an order-of-magnitude higher sensitivity than the ^{2}H NMR measurement. Figure 1b illustrates the analysis of the transfer hydrodeuteration of 2-vinylnaphthalene (**6b**, **7b**, **8b**), where no misdeuteration reaction product is identified at the measurement sensitivity using the broadband MRR instrument.

After the initial analyses of the six reaction products depicted in Scheme 3 (these results are tabulated in the SI), a modified MRR analysis approach was developed to address some weaknesses in the application of MRR to the development of synthetic methodologies for selective deuteration chemistry. One issue with the CP-FTMW analysis is the possibility that the spectral signature of an isotopic impurity is missed because the quantum chemistry predictions of the rotational spectrum make it difficult to identify the spectrum when it is near the detection limit. The sample consumption for the analysis is also a potential limitation. The broadband MRR analysis initially performed for the products depicted in Scheme 3 consumed 60–100 mg to reach a detection limit of about 1% on the expected isotopic impurities. Finally, the measurement

https://doi.org/10.1021/jacs.1c00884
J. Am. Chem. Soc. 2021, 143, 7707–7718

Table 2. Isotopic Composition of the 2-Ethylnaphthalene Mixture Giving the Total Intensity for Eight Transitions of Each Conformer for the Four Chemically Distinct Isotopic Variants Observed in the Spectrum

d_0		d_1-benzylic		d_1-methyl		d_2-benzylic-methyl	
	280 μV	D19[a]	57.0 μV	D22	38.0 μV	D19 D22	8.17 μV
		D20	55.4 μV	D23	36.3 μV	D19 D23	8.72 μV
				D24	41.9 μV	D19 D24	7.82 μV
						D20 D22	9.25 μV
						D20 D23	9.38 μV
						D20 D24	10.6 μV
Total	280 μV		112.4 μV		116.2 μV		53.9 μV
%	49.8		20.0		20.7		9.6
d_1-methyl conformers:				Mean: 38.7 μV		σ = 2.84 μV	
d_2-benzylic-methyl conformers:				Mean: 8.99 μV		σ = 0.98 μV	

[a]The isotope labels, like D19, refer to the atom labeling from the quantum chemistry geometry optimization as shown in the Supporting Information.

time is approximately 3 h. Shorter measurement times are needed to facilitate screening of reaction conditions to optimize the deuteration selectivity.

The new measurement approach combines broadband MRR spectroscopy to obtain the spectral signatures of all possible isotopic species accessible from the transfer hydrodeuteration chemistry, with high-throughput sample analysis performed on an IsoMRR instrument.[63] The IsoMRR instrument uses the tunable cavity-enhanced FTMW design introduced by Balle and Flygare.[64] The instrument employs coaxial injection of the sample through a solenoid valve mounted in the resonator mirror as introduced by Grabow, Stahl, and Dreizler to increase the measurement sensitivity.[65] The compact instrument design is based off the mini-FTMW instrument design from NIST.[66] The IsoMRR spectrometer has approximately an order-of-magnitude greater sensitivity than the broadband spectrometer for equal sample consumption. The instrument is also capable of performing high-throughput sample screening.[67] The trade-off of using a cavity-enhanced FTMW spectrometer is that the cavity resonator limits the measurement bandwidth to about 1 MHz. Due to the small bandwidth window, efficient use of the instrument relies on the availability of the transition frequencies of each isotopic species to be studied and these are supplied from the broadband analysis.

The sample analyzed by broadband MRR is prepared by performing the reaction with a 1:1 mixture of H and D reagents so that a "cocktail" of all possible reaction products is produced (eq 3). Once this sample is analyzed, the spectral signatures are used to set up a high-speed measurement script using a cavity-enhanced Fourier transform microwave (FTMW) spectrometer. This measurement methodology was tested on the isolated products from the Cu-catalyzed "cocktail" reactions performed with **5a**, **5b**, and **5d** shown in (eq 3) below:

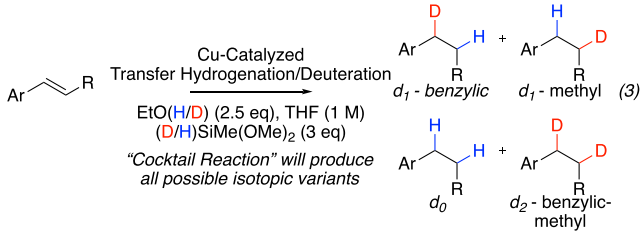

The analysis of the reaction mixture using the broadband CP-FTMW spectrometer is illustrated in Figure 2 for the Cu-catalyzed "cocktail" reaction of 2-vinylnaphthalene **5b**. Panels A and B show the spectrum for a commercial sample of ethylnaphthalene-d_0 for simplicity (this species is also the dominant species in the cocktail reaction mixture). Panel A shows the MRR spectrum in a small frequency range of the full 2−8 GHz measured spectrum. The rotational spectrum prediction from the equilibrium geometry and dipole moments obtained from the quantum chemistry geometry optimization is shown in blue and is a close match to the observed pattern. Panel B shows an expanded frequency region for two of the transitions in ethylnaphthalene-d_0. The assignment listed above each transition uses the usual notation in rotational spectroscopy that labels the energy levels J_{KaKc}.[54] The blue spectrum simulation is from quantum chemistry. The red simulation uses the experimental fit rotational constants which are given in the Supporting Information.

The spectral signatures of each deuterated 2-ethylnaphthalene species can be predicted to high accuracy using the theoretical equilibrium geometry and scale factors obtained from the theoretical and fit constants of ethylnaphthalene-d_0. This process is described in the Supporting Information and is a common analysis tool in rotational spectroscopy where it is used to identify ^{13}C (and other) isotopomers in natural abundance in structure determination.[68] The accuracy of this analysis is illustrated in Panel C where the predicted transitions of the $6_{16} - 5_{15}$ rotational transitions of the six conformers of the d_2-benzylic-methyl isotopomer are compared to the measured spectrum. The Supporting Information gives the comparison between the scaled rotational constant predictions and the experimental fit rotational constants for the 11 isotopic species identified in the spectrum. Agreement is on the order of 0.01%. Panel D shows the $J = 6 - J = 5$ spectral region of the reaction product mixture and the residual spectrum (blue) after all isotopic species (including the rotational spectra for the 12 singly substituted ^{13}C isotopomers of the dominant ethylnaphthalene-d_0 species) are cut from the spectrum. The only isotopomers identified in the spectrum are d_0, d_1-benzylic, d_1-methyl, and d_2-benzylic-methyl, and this is consistent with the proposed reaction products.

The broadband spectrum can be used to perform quantitative analysis of the reaction product mixture. To average fluctuations from the frequency-dependent electric field of the chirped excitation pulse, the total intensity of a set of rotational transitions is used. The analysis needs to include the spectral intensity from all conformers of a given isotopomer. The result using eight transitions in the 2-ethylnaphthalene spectrum is shown in Table 2. Analysis of the

https://doi.org/10.1021/jacs.1c00884
J. Am. Chem. Soc. 2021, 143, 7707−7718

Table 3. Comparison Between Calculated NMR Integration Using MRR Sample Composition and Measured NMR Integration

	Ethylbenzofuran		Ethylnaphthalene		Ethylbiphenyl		Ethylbiphenyl (D-enhanced)	
NMR Resonance	MRR[a]	NMR	MRR	NMR	MRR	NMR	MRR	NMR
Methyl ^{1}H	2.72(1)	2.69	2.70(2)	2.71	2.69(2)	2.73	2.46(2)	2.46
Benzylic ^{1}H	1.45(2)	1.43	1.70(2)	1.71	1.66(2)	1.69	1.31(2)	1.29
Methyl ^{2}H	0.28(1)	0.31	0.30(2)	0.29	0.31(2)	0.27	0.54(2)	0.52
Benzylic ^{2}H	0.55(2)	0.57	0.30(2)	0.28	0.34(2)	0.30	0.69(2)	0.71
Mean Absolute Percent Difference (^{1}H Only):					1.0%			
Mean Absolute Percent Difference (All):					4.0%			

[a]The MRR integrations give the 1σ uncertainty derived from the composition uncertainty.

Table 4. Comparison of Sample Composition Analysis by Broadband and Cavity-Enhanced MRR Spectroscopy

Ethylbenzofuran	Run 1	Run 2	Run 3	IsoMRR[a]	CP-FTMW[b]	|Difference|
d_0	29.4%	30.3%	30.0%	29.9(0.45)	34(2.4)	4.1%
d_1-benzylic	33.7%	31.9%	31.8%	32.6(1.1)	38(2.1)	5.4%
d_1-methyl	13.4%	14.3%	15.1%	14.3(0.85)	11.4(0.8)	2.9%
d_2-methyl-benzylic	23.5%	23.5%	23.1%	23.4(0.23)	16.8(0.9)	6.6%
Ethylnaphthalene	Run 1	Run 2	Run 3	IsoMRR[a]	CP-FTMW[b]	|Difference|
d_0	55.2%	54.3%	54.2%	54.6(0.55)	50(2.7)	4.6%
d_1-benzylic	14.9%	15.1%	14.8%	14.9(0.15)	20(1.6)	5.1%
d_1-methyl	21.0%	21.5%	21.4%	21.3(0.26)	21(1.4)	0.3%
d_2-methyl-benzylic	9.0%	9.2%	9.6%	9.3(0.31)	9.6(0.6)	0.3%
Ethylbiphenyl	Run 1	Run 2		IsoMRR[a]	CP-FTMW[b]	|Difference|
d_0	49.7%	51.7%		50.7(1.4)	46(2.7)	4.9%
d_1-benzylic	18.7%	18.0%		18.4(0.49)	23(1.7)	4.7%
d_1-methyl	20.8%	20.3%		20.6(0.35)	21(1.4)	0.4%
d_2-methyl-benzylic	10.8%	9.9%		10.4(0.64)	10.6(0.7)	0.2%

[a]The IsoMRR results are the mean value of the replicate measurements with a 1σ sample standard deviation reported in parentheses. [b]The measurement uncertainty reported for the CP-FTMW broadband measurements is a 1σ standard deviation determined by assuming that there is a 10% relative uncertainty in the intensity measurement ($(\sigma_I/I) = 0.1$) for each rotationally distinct species in the sample mixture.

results for the 5-ethylbenzofuran and ethylbiphenyl product mixtures are included in the Supporting Information.

There are two important spectroscopy details in the analysis. First, the analysis assumes that the dipole moment is the same for all isotopic variants so that the total spectral intensity is directly proportional to the isotopic composition. The dipole moment differs for the different species through two effects. Deuterium substitution reorients the principal axis system for molecular rotation and changes the components of the dipole moment vector in this axis system. This effect can be calculated from the equilibrium geometry and is negligible in the samples analyzed in this work. For example, the value of μ_a^2—the square of the component of the electric dipole moment along the a-principal axis which governs the intensities of the transitions used in the analysis—varies by just 0.1% for the 12 rotationally distinct structures analyzed for ethylnaphthalene. The dipole moment also changes magnitude upon deuteration from changes in the zero-point motion of the C−H bond. These effects have been measured, and the bond dipole changes are on the order of 0.01 D which is small compared to the dipole moments of the molecules in this study (>0.4 D).[69] The second spectroscopy issue that can affect the quantitative analysis is the presence of nuclear quadrupole hyperfine splitting in the spectrum from the deuterium nucleus ($I = 1$). The quantitative analysis uses only a-type rotational transitions where the hyperfine structure is small compared to the line width and can, therefore, be neglected.

The accuracy of the sample composition analysis by broadband MRR spectroscopy has been validated by comparison to integration of specific resonances in the ^{1}H and ^{2}H NMR spectra of the reaction mixture. It is important to note that NMR spectroscopy cannot analyze the composition of this reaction mixture. The resonances used in the NMR analysis are assigned to the benzylic and methyl protons. However, the reaction mixture contains three isotopic species (d_1-benzylic, d_1-methyl, and d_2-benzylic-methyl) that contribute to the two resonances making it impossible to analyze the sample composition by NMR. This simple example illustrates the limitations of NMR spectroscopy for reaction product analysis in deuteration chemistry. MRR can perform the analysis because all isotopic variants have a unique spectral signature.

The accuracy of the MRR composition is assessed by calculating the expected NMR integration for the sample using the MRR results reported in Table 2 (2-ethylnaphthalene) and the Supporting Information (5-ethylbenzofuran and ethylbiphenyl). For example, the integration of the methyl proton resonance using the fractional composition of the sample is

$$^1\text{H Methyl} = (f_{d0})*3 + (f_{d1\text{-benzylic}})*3 + (f_{d1\text{-methyl}})*2 + (f_{d2\text{-benzylic-methyl}})*2 \quad (4)$$

The quantitative comparison between MRR and NMR resonance integrations is presented in Table 3 for four reaction mixtures that were analyzed in this work (this includes a second ethylbiphenyl (D-enhanced)mixture where the ratio of H/D reagents was 1:2 to increase the contribution from the deuterated species). The mean absolute percent difference between the results is 1% for the ^{1}H integration.

https://doi.org/10.1021/jacs.1c00884
J. Am. Chem. Soc. 2021, 143, 7707−7718

The reaction product mixtures prepared using a 1:1 ratio of H/D reagents were subsequently analyzed using the IsoMRR instrument. A measurement script was designed to permit detection of the four chemically distinct isotopic species at the 1% level for each of the three analytes. These scripts are described in the Supporting Information. The measurement script does not need to make measurements for all conformers of a given isotopomer. As shown in Table 2, equal amounts of the conformers are observed in the spectrum (within a 10% intensity uncertainty) so that the measurement can use just one and then apply the statistical factor to get the total sample composition for the isotopomer. The sample composition from the IsoMRR measurements is compared to the CP-FTMW analysis in Table 4.

The composition analysis from the two MRR instruments are in good agreement with a percentage variation of about 5%. However, the 5% accuracy has little practical importance in applications of high-throughput screening where the measurement precision (better than 1%) is needed to determine which samples have higher purity. The lower accuracy of the IsoMRR measurements results from the instrument design which uses a cavity-resonator with high quality factor (Q) to enhance the measurement sensitivity. There has been no attempt to correct for frequency-dependent variation in the cavity Q in these measurements (although transitions in a narrow frequency range are used to minimize variations in the cavity Q). In practice, the IsoMRR measurements can achieve both high precision and accuracy by calibrating the instrument response using a reference sample that has been analyzed by broadband rotational spectroscopy where the quantitative accuracy is demonstrated in Table 3.

The more important feature of the IsoMRR measurements is the repeatability in back-to-back analysis runs which is about 1%. This measurement precision shows that the technique would be able to reliably detect changes in the sample composition for high-throughput screening of reaction conditions. The IsoMRR measurement for 2-ethylnaphthalene and 5-ethylbenzofuran uses 2.5 mg of sample (for ethylbiphenyl where the spectrum is weaker, the sample consumption is 5 mg). The measurement time is approximately 10 min (20 min for ethylbiphenyl). Both performance metrics are order-of-magnitude improvements over sample analysis by broadband MRR using the CP-FTMW spectrometer.

The IsoMRR instrument was also used to analyze the reaction products depicted in Scheme 3. These measurements detected the presence of the d_1-methyl isotopomer in ethylnaphthalene that was not observable in the broadband analysis (Figure 1b): (94.8% d_1-benzylic (**6b**), 4.4% d_0 (**8b**), 0.8% d_1-methyl (**7b**), <0.6% d_2 (nd)). For ethylbenzofuran, the IsoMRR analysis agrees with the broadband analysis within the performance comparison limits of Table 4: (95.1% d_1-benzylic (**6d**), 1.7% d_0 (**8d**), 3.2% d_1-methyl (**7d**), <0.7% d_2 (nd)). For ethylbiphenyl, only the underdeuterated isotopic impurity was detected: (98.4% d_1-benzylic (**6a**), 1.6% d_0 (**8a**), <0.7% d_1-methyl (**7a**) (nd), <1.3% d_2 (nd)). In addition, three separate preparations of ethylbiphenyl using the optimized chemistry were analyzed. The only two species detected were the desired d_1-benzylic and the underdeuterated d_0 isotopologue. The amount of d_0 (**8a**) impurity in the three samples was 1.6%, 2.3%, and 1.8%.

4. CONCLUSIONS

In summary, a highly regioselective alkene transfer hydrodeuteration for the synthesis of deuterated small molecules where deuterium is incorporated at the benzylic position is reported. The Cu-catalyzed reaction is able to incorporate both an H and a D across an alkene with high levels of precision. This mild protocol can be carried out across a broad range of aryl alkene substrates, including those containing heterocycles and reduceable functionality. A detailed characterization of six reaction product mixtures was performed using molecular rotational resonance spectroscopy. MRR provides a general method to perform isotopomer composition analysis of deuteration reactions. The following advantages of MRR spectroscopy for characterization of isotopic products were outlined during the characterization of six isotopic product mixtures from the alkene transfer hydrodeuteration reaction. (1) Isotopomers have distinct MRR spectra that can be predicted to high accuracy from the theoretical equilibrium geometry from quantum chemistry. This feature makes it possible to identify the isotopomers with high confidence without the need for reference samples. (2) Instruments for MRR provide high spectral resolution so that isotopologue and isotopomer mixtures can be quantitatively analyzed without issues arising from signal overlap. (3) High-throughput analysis is possible using cavity-enhanced FTMW spectrometers making it possible to screen a wide range of reaction conditions for isotopic reactions. These capabilities were especially important for analyzing the reaction products from the reported Cu-catalyzed alkene transfer hydrodeuteration reaction. Reaction mixtures may contain three isotopic species (d_1-benzylic, d_1-methyl, and d_2-benzylic-methyl), and these contribute to two NMR resonances. This scenario made it challenging to analyze the sample composition by NMR. In addition to the enhanced sensitivity of MRR, the identification of the d_1-methyl isotopomer **7b** (the minor regioisomer from the transfer hydrodeuteration of 2-ethylnaphthalene) was possible. This species was not detected by NMR. Ultimately, using MRR spectroscopy to analyze the isotopic products formed from the reported highly regioselective Cu-catalyzed alkene transfer hydrodeuteration reaction led to the highest regioselectivities ever reported for this reaction. We anticipate that the advances reported for the selective hydrodeuteration chemistry and MRR spectroscopy will facilitate new reaction discovery in selective deuteration chemistry and expand the utility of deuterium-labeled organic compounds in applications that require the molecule has high deuterium content at precisely the desired site.

■ ASSOCIATED CONTENT

Supporting Information

The Supporting Information is available free of charge at https://pubs.acs.org/doi/10.1021/jacs.1c00884.

General information, procedures for transfer hydrodeuteration and synthesis of starting materials along with ^{1}H NMR, ^{2}H NMR, ^{11}B NMR and ^{13}C NMR spectra, and HRMS and IR data of all newly characterized products. Molecular rotational resonance spectroscopy data for compounds in Scheme 3 is also included. (PDF)

https://doi.org/10.1021/jacs.1c00884
J. Am. Chem. Soc. 2021, 143, 7707−7718

AUTHOR INFORMATION

Corresponding Author

Joseph R. Clark − *Department of Chemistry, Marquette University, Milwaukee, Wisconsin 53233-1881, United States;* orcid.org/0000-0002-3081-5732; Email: joseph.r.clark@marquette.edu

Authors

Zoua Pa Vang − *Department of Chemistry, Marquette University, Milwaukee, Wisconsin 53233-1881, United States*

Albert Reyes − *Department of Chemistry, Marquette University, Milwaukee, Wisconsin 53233-1881, United States*

Reilly E. Sonstrom − *Department of Chemistry, University of Virginia, Charlottesville, Virginia 22904-4319, United States;* orcid.org/0000-0003-0497-6660

Martin S. Holdren − *Department of Chemistry, University of Virginia, Charlottesville, Virginia 22904-4319, United States*

Samantha E. Sloane − *Department of Chemistry, Marquette University, Milwaukee, Wisconsin 53233-1881, United States*

Isabella Y. Alansari − *Department of Chemistry, Marquette University, Milwaukee, Wisconsin 53233-1881, United States*

Justin L. Neill − *BrightSpec, Inc., Charlottesville, Virginia 22903, United States;* orcid.org/0000-0003-0964-3275

Brooks H. Pate − *Department of Chemistry, University of Virginia, Charlottesville, Virginia 22904-4319, United States*

Complete contact information is available at: https://pubs.acs.org/10.1021/jacs.1c00884

Author Contributions

‖Z.P.V. and A.R. contributed equally.

Funding

Financial support for this work was provided by Marquette University. MRR analysis of the isotopic impurities was performed with support from the National Science Foundation Chemical Measurement and Imaging Program under grant NSF-1904686.

Notes

The authors declare the following competing financial interest(s): Brooks H. Pate has founders equity in BrightSpec which commercializes applications of rotational spectroscopy in chemical analysis. Reilly Sonstrom and Justin Neill also have equity in BrightSpec.

ACKNOWLEDGMENTS

A.R. is grateful for a 2020 Eugene Kroeff summer research fellowship and 2020 Ronald E. McNair summer research fellowship. I.A. is grateful for a 2020 James Moyer summer research fellowship.

REFERENCES

(1) Atzrodt, J.; Derdau, V. Pd- and Pt-catalyzed H/D exchange methods and their application for internal MS standard preparation from a Sanofi-Aventis perspective. *J. Labelled Compd. Radiopharm.* **2010**, *53*, 674−685.

(2) Qin, M.; Qiao, H.-q.; Yuan, Y.-j.; Shao, Q. A quantitative LC-MS/MS method for simultaneous determination of deuvortioxetine, vortioxetine and their carboxylic acid metabolite in rat plasma, and its application to a toxicokinetic study. *Anal. Methods* **2018**, *10*, 1023−1031.

(3) Iglesias, J.; Sleno, L.; Volmer, D. A. Isotopic Labeling of Metabolites in Drug Discovery Applications. *Curr. Drug Metab.* **2012**, *13*, 1213−1225.

(4) Meek, S. J.; Pitman, C. L.; Miller, A. J. M. Deducing Reaction Mechanism: A Guide for Students, Researchers, and Instructors. *J. Chem. Educ.* **2016**, *93*, 275−286.

(5) Anslyn, E. V.; Dougherty, D. A. *Modern physical organic chemistry*; University Science Books: 2006; pp 424−441.

(6) Simmons, E. M.; Hartwig, J. F. On the Interpretation of Deuterium Kinetic Isotope Effects in C-H Bond Functionalizations by Transition-Metal Complexes. *Angew. Chem., Int. Ed.* **2012**, *51*, 3066−3072.

(7) Giagou, T.; Meyer, M. P. Kinetic Isotope Effects in Asymmetric Reactions. *Chem. - Eur. J.* **2010**, *16*, 10616−10628.

(8) Atzrodt, J.; Derdau, V.; Kerr, W. J.; Reid, M. Deuterium- and Tritium-Labelled Compounds: Applications in the Life Sciences. *Angew. Chem., Int. Ed.* **2018**, *57*, 1758−1784.

(9) Jarling, R.; Sadeghi, M.; Drozdowska, M.; Lahme, S.; Buckel, W.; Rabus, R.; Widdel, F.; Golding, B. T.; Wilkes, H. Stereochemical Investigations Reveal the Mechanism of the Bacterial Activation of n-Alkanes without Oxygen. *Angew. Chem., Int. Ed.* **2012**, *51*, 1334−1338.

(10) Klinman, J. P. A new model for the origin of kinetic hydrogen isotope effects. *J. Phys. Org. Chem.* **2010**, *23*, 606−612.

(11) Schwab, J. M. Stereochemistry of an enzymic Baeyer-Villiger reaction. Application of deuterium NMR. *J. Am. Chem. Soc.* **1981**, *103*, 1876−1878.

(12) Battersby, A. R.; Gutman, A. L.; Fookes, C. J. R.; Günther, H.; Simon, H. Stereochemistry of formation of methyl and ethyl groups in bacteriochlorophyll a. *J. Chem. Soc., Chem. Commun.* **1981**, 645−647.

(13) Leinberger, R.; Rétey, A.; Hull, W. E.; Simon, H. Steric Course of the NIH Shift in the Enzymic Formation of Homogentisic Acid. *Eur. J. Biochem.* **1981**, *117*, 311−318.

(14) Lüthy, J.; Rétey, J.; Arigoni, D. Asymmetric Methyl Groups: Preparation and Detection of Chiral Methyl Groups. *Nature* **1969**, *221*, 1213−1215.

(15) White, R. E.; Miller, J. P.; Favreau, L. V.; Bhattacharyya, A. Stereochemical dynamics of aliphatic hydroxylation by cytochrome P-450. *J. Am. Chem. Soc.* **1986**, *108*, 6024−6031.

(16) Shapiro, S.; Piper, J. U.; Caspi, E. Steric course of hydroxylation at primary carbon atoms. Biosynthesis of 1-octanol from (1R)- and (1S)-[1−3H,2H,1H; 1−14C]octane by rat liver microsomes. *J. Am. Chem. Soc.* **1982**, *104*, 2301−2305.

(17) Nelson, S. D.; Trager, W. F. The Use of Deuterium Isotope Effects to Probe the active site properties, Mechanism of Cytochrom P450-Catalyzed Reactions, and Mechanisms of Metabolically Dependent Toxicity. *Drug Metab. Dispos.* **2003**, *31*, 1481−1497.

(18) Pirali, T.; Serafini, M.; Cargnin, S.; Genazzani, A. A. Applications of Deuterium in Medicinal Chemistry. *J. Med. Chem.* **2019**, *62*, 5276−5297.

(19) Gant, T. G. Using Deuterium in Drug Discovery: Leaving the Label in the Drug. *J. Med. Chem.* **2014**, *57*, 3595−3611.

(20) Meanwell, N. A. Synopsis of Some Recent Tactical Application of Bioisosteres in Drug Design. *J. Med. Chem.* **2011**, *54*, 2529−2591.

(21) Stepan, A. F.; Mascitti, V.; Beaumont, K.; Kalgutkar, A. S. Metabolism-guided drug design. *MedChemComm* **2013**, *4*, 631−652.

(22) Belleau, B.; Burba, J.; Pindell, M.; Reiffenstein, J. Effect of Deuterium Substitution in Sympathomimetic Amines on Adrenergic Responses. *Science* **1961**, *133*, 102−104.

(23) Harbeson, S. L.; Tung, R. D. Deuterium Medicinal Chemistry: A New Approach to Drug Discovery and Development. *Medchem News* **2014**, *24*, 8−22.

(24) Schmidt, C. First deuterated drug approved. *Nat. Biotechnol.* **2017**, *35*, 493−494.

(25) Ludwig, J. R.; Schindler, C. S. Catalyst: Sustainable Catalysis. *Chem.* **2017**, *2*, 313−316.

(26) Zhou, Q.-L. Transition-Metal Catalysis and Organocatalysis: Where Can Progress Be Expected? *Angew. Chem., Int. Ed.* **2016**, *55*, 5352−5353.

(27) Atzrodt, J.; Derdau, V.; Fey, T.; Zimmermann, J. The Renaissance of H/D Exchange. *Angew. Chem., Int. Ed.* **2007**, *46*, 7744−7765.

(28) Atzrodt, J.; Derdau, V.; Kerr, W. J.; Reid, M. C−H Functionalisation for Hydrogen Isotope Exchange. *Angew. Chem., Int. Ed.* **2018**, *57*, 3022−3047.
(29) Puleo, T. R.; Strong, A. J.; Bandar, J. S. Catalytic α-Selective Deuteration of Styrene Derivatives. *J. Am. Chem. Soc.* **2019**, *141*, 1467−1472.
(30) Karlsson, S.; Hallberg, A.; Gronowitz, S. Hydrozirconation of (E)-3-methoxy-1-phenyl-1-propene and (E)-3-phenyl-2-propenol. *J. Organomet. Chem.* **1991**, *403*, 133−144.
(31) Czeskis, B.; Elmore, C. S.; Haight, A.; Hesk, D.; Maxwell, B. D.; Miller, S. A.; Raglione, T.; Schildknegt, K.; Traverse, J. F.; Wang, P. Deuterated Active Pharmaceutical Ingredients: A Science-Based Proposal for Synthesis, Analysis, and Control. Part 1: Framing the Problem. *J. Labelled Compd. Radiopharm.* **2019**, *62*, 690−694.
(32) Wang, D.; Astruc, D. The Golden Age of Transfer Hydrogenation. *Chem. Rev.* **2015**, *115*, 6621−6686.
(33) Korytiaková, E.; Thiel, N. O.; Pape, F.; Teichert, J. F. Copper(i)-Catalysed Transfer Hydrogenations with Ammonia Borane. *Chem. Commun.* **2017**, *53*, 732−735.
(34) Chatterjee, I.; Oestreich, M. Brønsted Acid-Catalyzed Transfer Hydrogenation of Imines and Alkenes Using Cyclohexa-1,4-dienes as Dihydrogen Surrogates. *Org. Lett.* **2016**, *18*, 2463−2466.
(35) Lau, S.; Gasperini, D.; Webster, R. L., Amine-Boranes as Transfer Hydrogenation and Hydrogenation Reagents: A Mechanistic Perspective. *Angew. Chem., Int. Ed.* **2021**, DOI: 10.1002/anie.202010835.
(36) Semba, K.; Fujihara, T.; Xu, T.; Terao, J.; Tsuji, Y. Copper-Catalyzed Highly Selective Semihydrogenation of Non-Polar Carbon-Carbon Multiple Bonds using a Silane and an Alcohol. *Adv. Synth. Catal.* **2012**, *354*, 1542−1550.
(37) Whittaker, A. M.; Lalic, G. Monophasic Catalytic System for the Selective Semireduction of Alkynes. *Org. Lett.* **2013**, *15*, 1112−1115.
(38) Kaicharla, T.; Zimmermann, B. M.; Oestreich, M.; Teichert, J. F. Using Alcohols as Simple H_2-Equivalents for Copper-Catalysed Transfer Semihydrogenations of Alkynes. *Chem. Commun.* **2019**, *55*, 13410−13413.
(39) Okuhara, T.; Tanaka, K.-I. Orientation in the Addition of HD to Butadiene on MoS_2. *J. Chem. Soc., Chem. Commun.* **1976**, 199−200.
(40) Okuhara, T.; Kondo, T.; Tanaka, K. Oriented Adsorption of Hydrogen Deuteride on Zinc Oxide and Addition to Butadiene. *J. Phys. Chem.* **1977**, *81*, 808−809.
(41) Espinal-Viguri, M.; Neale, S. E.; Coles, N. T.; Macgregor, S. A.; Webster, R. L. Room Temperature Iron-Catalyzed Transfer Hydrogenation and Regioselective Deuteration of Carbon−Carbon Double Bonds. *J. Am. Chem. Soc.* **2019**, *141*, 572−582.
(42) Wang, Y.; Cao, X.; Zhao, L.; Pi, C.; Ji, J.; Cui, X.; Wu, Y. Generalized Chemoselective Transfer Hydrogenation/Hydrodeuteration. *Adv. Synth. Catal.* **2020**, *362*, 4119−4129.
(43) Linford-Wood, T. G.; Coles, N. T.; Webster, R. L. Room temperature iron catalyzed transfer hydrogenation using *n*-butanol and poly(methylhydrosiloxane). *Green Chem.* **2021**, *23*, 2703−2709.
(44) Walker, J. C. L.; Oestreich, M. Regioselective Transfer Hydrodeuteration of Alkenes with a Hydrogen Deuteride Surrogate Using $B(C_6F_5)_3$ Catalysis. *Org. Lett.* **2018**, *20*, 6411−6414.
(45) Li, L.; Hilt, G. Regiodivergent DH or HD Addition to Alkenes: Deuterohydrogenation versus Hydrodeuterogenation. *Org. Lett.* **2020**, *22*, 1628−1632.
(46) Sloane, S. E.; Reyes, A.; Vang, Z. P.; Li, L.; Behlow, K. T.; Clark, J. R. Copper-Catalyzed Formal Transfer Hydrogenation/Deuteration of Aryl Alkynes. *Org. Lett.* **2020**, *22*, 9139−9144.
(47) Liu, R. Y.; Buchwald, S. L. CuH-Catalyzed Olefin Functionalization: From Hydroamination to Carbonyl Addition. *Acc. Chem. Res.* **2020**, *53*, 1229−1243.
(48) Zhu, S.; Niljianskul, N.; Buchwald, S. L. Enantio- and Regioselective CuH-Catalyzed Hydroamination of Alkenes. *J. Am. Chem. Soc.* **2013**, *135*, 15746−15749.
(49) Miki, Y.; Hirano, K.; Satoh, T.; Miura, M. Copper-Catalyzed Intermolecular Regioselective Hydroamination of Styrenes with Polymethylhydrosiloxane and Hydroxylamines. *Angew. Chem., Int. Ed.* **2013**, *52*, 10830−10834.
(50) Sorádová, Z.; Šebesta, R. Enantioselective Cu-Catalyzed Functionalizations of Unactivated Alkenes. *ChemCatChem* **2016**, *8*, 2581−2588.
(51) Mohr, J.; Oestreich, M. Balancing C = C Functionalization and C = O Reduction in Cu-H Catalysis. *Angew. Chem., Int. Ed.* **2016**, *55*, 12148−12149.
(52) Vitaku, E.; Smith, D. T.; Njardarson, J. T. Analysis of the Structural Diversity, Substitution Patterns, and Frequency of Nitrogen Heterocycles among U.S. FDA Approved Pharmaceuticals. *J. Med. Chem.* **2014**, *57*, 10257−10274.
(53) Taylor, R. D.; MacCoss, M.; Lawson, A. D. G. Rings in Drugs. *J. Med. Chem.* **2014**, *57*, 5845−5859.
(54) W. Gordy, R. L. C. *Microwave Molecular Spectra*, 3rd ed.; Knovel, 1984; Chapter VII, pp 227−296.
(55) Smith, J. A.; Wilson, K. B.; Sonstrom, R. E.; Kelleher, P. J.; Welch, K. D.; Pert, E. K.; Westendorff, K. S.; Dickie, D. A.; Wang, X.; Pate, B. H.; Harman, W. D. Preparation of cyclohexene isotopologues and stereoisotopomers from benzene. *Nature* **2020**, *581*, 288−293.
(56) Grimme, S.; Steinmetz, M. Effects of London dispersion correction in density functional theory on the structures of organic molecules in the gas phase. *Phys. Chem. Chem. Phys.* **2013**, *15*, 16031−16042.
(57) Lee, K. L. K.; McCarthy, M. Bayesian Analysis of Theoretical Rotational Constants from Low-Cost Electronic Structure Methods. *J. Phys. Chem. A* **2020**, *124*, 898−910.
(58) Brown, G. G.; Dian, B. C.; Douglass, K. O.; Geyer, S. M.; Shipman, S. T.; Pate, B. H. A broadband Fourier transform microwave spectrometer based on chirped pulse excitation. *Rev. Sci. Instrum.* **2008**, *79*, No. 053103.
(59) Neill, J. L.; Shipman, S. T.; Alvarez-Valtierra, L.; Lesarri, A.; Kisiel, Z.; Pate, B. H. Rotational spectroscopy of iodobenzene and iodobenzene−neon with a direct digital 2−8 GHz chirped-pulse Fourier transform microwave spectrometer. *J. Mol. Spectrosc.* **2011**, *269*, 21−29.
(60) Pérez, C.; Lobsiger, S.; Seifert, N. A.; Zaleski, D. P.; Temelso, B.; Shields, G. C.; Kisiel, Z.; Pate, B. H. Broadband Fourier transform rotational spectroscopy for structure determination: The water heptamer. *Chem. Phys. Lett.* **2013**, *571*, 1−15.
(61) Armstrong, D. W.; Talebi, M.; Thakur, N.; Wahab, M. F.; Mikhonin, A. V.; Muckle, M. T.; Neill, J. L. A Gas Chromatography-Molecular Rotational Resonance Spectroscopy Based System of Singular Specificity. *Angew. Chem., Int. Ed.* **2020**, *59*, 192−196.
(62) Frisch, M. J.; Trucks, G. W.; Schlegel, H. B.; Scuseria, G. E.; Robb, M. A.; Cheeseman, J. R.; Scalmani, G.; Barone, V.; Petersson, G. A.; Nakatsuji, H.; Li, X.; Caricato, M.; Marenich, A. V.; Bloino, J.; Janesko, B. G.; Gomperts, R.; Mennucci, B.; Hratchian, H. P.; Ortiz, J. V.; Izmaylov, A. F.; Sonneberg, J. L.; Williams-Young, D.; Ding, F.; Lipparini, F.; Egidi, F.; Goings, J.; Peng, B.; Petrone, A.; Henderson, T.; Ranasinghe, D.; Zakrzewski, V. G.; Gao, J.; Rega, N.; Zheng, G.; Liang, W.; Hada, M.; Ehara, M.; Toyota, K.; Fukuda, R.; Hasegawa, J.; Ishida, M.; Nakajima, T.; Honda, Y.; Kitao, O.; Nakai, H.; Vreven, T.; Throssell, K.; Montgomery, J. A., Jr.; Peralta, J. E.; Ogliaro, F.; Bearpark, M. J.; Heyd, J. J.; Brothers, E. N.; Kudin, K. N.; Staroverov, V. N.; Keith, T. A.; Kobayashi, R.; Normand, J.; Raghavachari, K.; Rendell, A. P.; Burat, J. C.; Iyengar, S. S.; Tomasi, J.; Cossi, M.; Millam, J. M.; Klene, M.; Adamo, C.; Cammi, R.; Ochterski, J. W.; Martin, R. L.; Morokuma, K.; Farkas, O.; Foresman, J. B.; Fox, D. J. *Gaussian 16*, rev. C.01; Gaussian Inc.: Wallingford, CT, 2016.
(63) The IsoMRR instrument is available from BrightSpec Inc.
(64) Balle, T. J.; Flygare, W. H. Fabry−Perot cavity pulsed Fourier transform microwave spectrometer with a pulsed nozzle particle source. *Rev. Sci. Instrum.* **1981**, *52*, 33−45.
(65) Grabow, J.; Stahl, W.; Dreizler, H. A multioctave coaxially oriented beam-resonator arrangement Fourier-transform microwave spectrometer. *Rev. Sci. Instrum.* **1996**, *67*, 4072−4084.
(66) Suenram, R. D.; Grabow, J. U.; Zuban, A.; Leonov, I. A portable, pulsed-molecular-beam, Fourier-transform microwave spec-

https://doi.org/10.1021/jacs.1c00884
J. Am. Chem. Soc. 2021, 143, 7707−7718

trometer designed for chemical analysis. *Rev. Sci. Instrum.* **1999**, *70*, 2127−2135.
(67) Neill, J. L.; Mikhonin, A. V.; Chen, T.; Sonstrom, R. E.; Pate, B. H. Rapid Quantitation of Isomeric and Dehalogenated Impurities in Pharmaceutical Raw Materials Using MRR Spectroscopy. *J. Pharm. Biomed. Anal.* **2020**, *189*, 113474.
(68) Gordy, R. L. C. W. *Microwave Molecular Spectra*, 3rd ed.; Knovel, 1984; Chapter XIII, pp 647−724.
(69) Fliege, E.; Dreizler, H. Investigation of the Stark Shift of the Benzene-d_1 l_{01} - 0_{00} Rotational Transition by Microwave Fourier Transform Spectroscopy. *Z. Naturforsch., A: Phys. Sci.* **1987**, *42a*, 72−78.

https://doi.org/10.1021/jacs.1c00884
J. Am. Chem. Soc. 2021, 143, 7707−7718